Molecular Crystals and Liquid Crystals

Publication details, including instructions for authors and subscription information:
http://www.tandfonline.com/loi/gmcl20

SYNTHESIS AND MESOMORPHIC PROPERTIES OF SCHIFF BASE ESTERS ORTHO-HYDROXY-PARA-ALKYLOXYBENZYLIDENE-PARA-SUBSTITUTED ANILINES

Guan-Yeow Yeap* [a], Sie-Tiong Ha [a], Phaik-Leng Lim [a], Peng-Lim Boey [a], Wan Ahmad Kamil Mahmood [a], Masato M. Ito [b] & Shigeki Sanehisa [b]

[a] School of Chemical Sciences, Universiti Sains Malaysia, 11800 Minden, Penang, Malaysia

[b] Soka University, Hachioji, Tokyo, Japan, 192-8577

Version of record first published: 02 Sep 2010

To cite this article: Guan-Yeow Yeap*, Sie-Tiong Ha, Phaik-Leng Lim, Peng-Lim Boey, Wan Ahmad Kamil Mahmood, Masato M. Ito & Shigeki Sanehisa (2004): SYNTHESIS AND MESOMORPHIC PROPERTIES OF SCHIFF BASE ESTERS ORTHO-HYDROXY-PARA-ALKYLOXYBENZYLIDENE-PARA-SUBSTITUTED ANILINES, Molecular Crystals and Liquid Crystals, 423:1, 73-84

To link to this article: http://dx.doi.org/10.1080/15421400490494508

Mol. Cryst. Liq. Cryst., Vol. 423, pp. 73–84, 2004

ISSN: 1542-1406 print/1563-5287 online
DOI: 10.1080/15421400490494508

Taylor & Francis
Taylor & Francis Group

SYNTHESIS AND MESOMORPHIC PROPERTIES OF SCHIFF BASE ESTERS *ORTHO*-HYDROXY-*PARA*-ALKYLOXYBENZYLIDENE-*PARA*-SUBSTITUTED ANILINES

Guan-Yeow Yeap, Sie-Tiong Ha, Phaik-Leng Lim, Peng-Lim Boey, and Wan Ahmad Kamil Mahmood*
School of Chemical Sciences, Universiti Sains Malaysia, 11800 Minden, Penang, Malaysia

Masato M. Ito and Shigeki Sanehisa
Faculty of Engineering, Soka University, Hachioji, Tokyo 192-8577, Japan

A series of new compounds o-*n-hydroxy*-p-*n-hexadecanoyloxybenzylideneaniline and its substituted derivatives was synthesized from the esterification of palmitic acid with intermediary Schiff bases, which posssess various terminal substituents X (X = H, F, Cl, Br, OCH_3, CH_3, and C_2H_5). All compounds possess mesomorphic properties wherein compounds with X = H, F, Cl, Br, and OCH_3 exhibit smectic A (SmA) phases and those with terminal substituents CH_3 and C_2H_5 are monotropic liquid crystals showing smectic C phases (SmC). Correlation studies of the clearing temperature (T_c) of the title compounds and polarizability related to mesophase stability and molecular anisotropy are reported.*

Keywords: clearing temperature; mesophase stability; molecular anisotropy; *o*-n-hydroxy-*p*-n-hexadecanoyloxybenzylideneaniline; palmitic acid; Schiff bases

INTRODUCTION

The pericarp of palm fruit is comprised of three layers, the exocarp (skin), mesocarp (outer pulp containing palm oil) and endocarp (a hard shell enclosing the kernel, which contains oil and carbohydrate reserves for the embryo) [1]. The major saturated fatty acid obtained from mesocarp

We are grateful to the Universiti Sains Malaysia and Malaysian Government for financial support through FRGS Grant No. 304/PKIMIA/670032 and IRPA (EA) Grant No. 305/PKIMIA/612923.

*Corresponding author. E-mail: gyyeap@usm.my

of palm oil is palmitic acid (44%), and this is balanced by 39% monounsaturated oleic acid and 11% polyunsaturated linoleic acid. The remainder consists of stearic (5%) and myristic (1%) acids. The composition is significantly different from palm kernel oil (obtained as coproduct during the processing of oil palm fruits), which is almost 85% saturated [1].

It has recently been found that palm oil is useful in fish diets, without negatively affecting growth and feed utilization efficiency [2,3]. In the field of liquid crystals, fatty acids and cholesterol from vegetable oils other than oil palm had also been reported well [4–15]. The synthesis of Schiff base esters, *p*-n-octadecanoyloxybenzylidene-*p*-substituted-anilines involving esterification of stearic acid and various substituted 4-hydroxybenzalideneanilines is further evidence of diversification of palm oil leading to the formation of liquid crystals [16,17].

In order to enhance further the rigidity of the core system in these Schiff base esters, we introduced the lateral hydroxy group into the aldehyde fragment, wherein the esterification occurred between the palmitic acid and 2,4-dihydroxybenzaldehyde prior to the condensation of aldehyde with nonsubstituted and various substituted anilines (Scheme 1). It has been claimed that the introduction of lateral polar hydroxyl group increased the molecular polarizability as well as higher clearing temperature. As such, a systematic study on the effect of substituent (H, F, Cl, Br, OCH_3, CH_3, and C_2H_5) in the aniline fragment of compounds **9–11** and their connectivities with the intramolecular interaction, lateral intermolecular interaction, and clearing temperatures were reported.

EXPERIMENTAL

4-Bromoaniline, 4-chloroaniline, 4-ethylaniline, and 4-dimethylaminopyridine (DMAP) were obtained from Merck (Germany). 2,4-Dihydroxybenzaldehyde and 4-fluoroaniline were purchased from Acros Organics (USA). While 4-methoxyaniline and dicyclohexylcarbodiimide (DCC) were purchased from Fluka Chemie (Switzerland), 4-methylaniline was obtained from Riedel-de Haen (Germany). Aniline was obtained from BDH (England). Palmitic acid used in this research was provided by Acidchem International Sdn. Bhd. (Malaysia). The purity of the palmitic acid is approximately 99%.

Melting points of the synthesized compounds were measured by Gallenkamp melting-point apparatus. Microanalyses were carried out on 2400 LS Series CHNS/O analyzers in The School of Chemical Sciences, Universiti Sains Malaysia, Penang, Malaysia. IR data were recorded using a Perkin Elmer 2000-FTIR spectrophotometer in the frequency range 4000–400 cm^{-1} with samples embedded in KBr discs. ^1H NMR and ^{13}C NMR spectra were recorded on a Bruker 400 MHz ultrashield spectrometer.

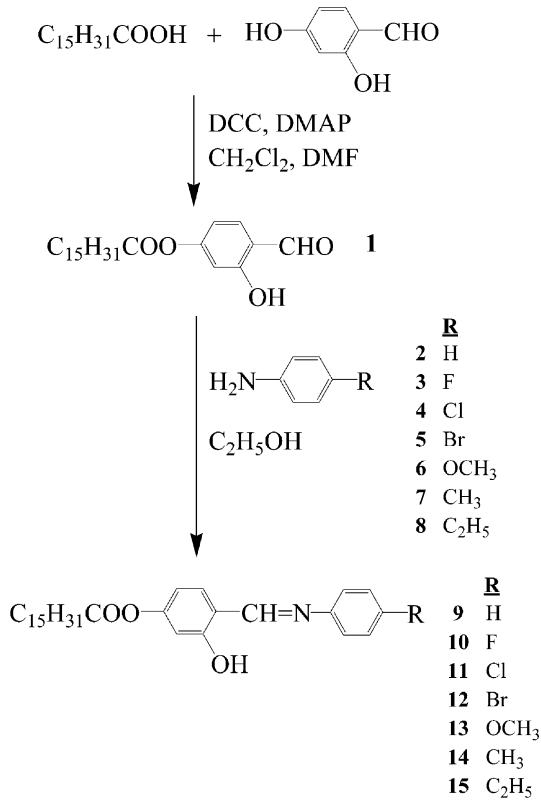

SCHEME 1 Synthetic routes towards the formation of intermediates and target compounds **9–15**.

Deuterated chloroform was used as solvent and tetramethylsilane (TMS) as internal standard. Thin layer chromatography analyses were perfomed using aluminium-backed silica gel plates (Merck 60 F254) and were examined under short-wave UV light.

The phase transition temperatures were measured by Shimadzu DSC-50 differential scanning calorimetry at heating and cooling rates of 5°C/min and −5°C/min, respectively. The optical microscopy studies were carried out with a Carl Zeiss polarizing microscope equipped with a Mettler FP52 hot stage. The textures of the compounds were observed by using polarized light with crossed polarizers, with the sample in thin film sandwiched between glass slide and cover.

Molecular modeling study was performed using the program ACD/Chemsketch Version 4.5. Geometrical optimization or energy minimization

of the molecules was performed in order to gain an appreciation of molecular shape and geometry. The structural conformation obtained was subsequently used in calculating the polarizability of each compound.

Synthesis

Synthesis of o-n-hydroxy-p-n-hexadecanoyloxybenzaldehyde, 1

This compound was synthesized via modified reaction described by Sudhakar et al. [18]. 2,4-Dihydroxybenzaldehyde (20 mole), palmitic acid (20 mmole), and DMAP (2 mmole) were dissolved in 60 ml mixture of dichloromethane (DCM) and dimethylformamide (DMF) and stirred at 0°C. To this solution 20 mmole of DCC dissolved in 20 ml of DCM was added dropwise and stirred at 0°C for 1 h and then stirred at room temperature for 3 h. Finally, the reaction mixture was filtered and DCM was removed from the filtrate by evaporation. The grey solid thus obtained was recrystallized with n-hexane, whereupon pure compound was formed. IR (KBr), 3441 cm^{-1} (OH), 1760 cm^{-1} (C=O of ester), 1690 cm^{-1} (CH=O).

Synthesis of o-n-hydroxy-p-n-hexadecanoyloxybenzylidene-p-aniline, 9

In a round-bottom flask, a mixture of **1** (1.0 mole), aniline (1.0 mole), and absolute ethanol or DCM (50 ml) was refluxed for 3 h with stirring. The reaction mixture was filtered and the solvent removed from the filtrate by evaporation. The yellowish crystalline was obtained after being recrystallized with absolute ethanol. Yield 79%. Elemental analysis found: C, 77.20; H, 9.25; N, 3.07. Calculated (for $C_{29}H_{41}NO_3$): C, 77.12; H, 9.15; N, 3.10. IR (KBr), 3436 cm^{-1} (OH), 2953, 2916, 2847 cm^{-1} (C−H aliphatic), 1756 cm^{-1} (C=O of ester), 1627 cm^{-1} (CH=N), 1594 cm^{-1} (C=C aromatic). ^{1}H NMR ($CDCl_3$), 0.91–0.94 ppm (CH_3), 1.25–2.57 ppm (CH_2), 6.71–7.46 ppm (Ar−H), 8.62 ppm (CH=N), 13.64 ppm (OH). ^{13}C NMR ($CDCl_3$), 14.56 ppm (CH_3), 23.14–34.86 ppm (CH_2), 110.85–162.99 ppm (Ar−C), 162.15 ppm (C=N), 172.11 (C=O of ester).

The preparation and characterization with the same procedures were carried out for compounds **10–15**. The analytical data were summarized as follows:

Synthesis of o-n-hydroxy-p-n-hexadecanoyloxybenzylidene-p-fluroaniline, 10

Yield 75%. Elemental analysis found: C, 74.03; H, 8.42; N, 2.93. Calculated (for $C_{29}H_{40}FNO_3$): C, 74.17; H, 8.55; N, 2.98. IR (KBr), 3443 cm^{-1} (OH), 2953, 2917, 2848 cm^{-1} (C−H aliphatic), 1758 cm^{-1} (C=O of ester), 1626 cm^{-1} (CH=N), 1608 cm^{-1} (C=C aromatic). ^{1}H NMR ($CDCl_3$), 0.88–0.92 ppm

(CH_3), 1.29–2.60 ppm (CH_2), 6.71–7.42 ppm (Ar−H), 8.59 ppm (CH=N), 13.42 ppm (OH). ^{13}C NMR ($CDCl_3$), 14.52 ppm (CH_3), 23.09–34.85 ppm (CH_2), 110.86–163.32 ppm (Ar−C), 161.96 ppm (C=N), 172.13 (C=O of ester).

Synthesis of o-n-hydroxy-p-n-hexadecanoyloxy-benzylidene-p-cloroaniline, 11

Yield 79%. Elemental analysis found: C, 71.58; H, 8.40; N, 2.87. Calculated (for $C_{29}H_{40}ClNO_3$): C, 71.66; H, 8.29; N, 2.88. IR (KBr), 3435 cm^{-1} (OH), 2951, 2917, 2847 cm^{-1} (C−H aliphatic), 1759 cm^{-1} (C=O of ester), 1625 cm^{-1} (CH=N), 1604 cm^{-1} (C=C aromatic). ^{1}H NMR ($CDCl_3$), 0.91–0.94 ppm (CH_3), 1.27–2.60 ppm (CH_2), 6.72–7.42 ppm (Ar−H), 8.58 ppm (CH=N), 13.15 ppm (OH). ^{13}C NMR ($CDCl_3$), 14.52 ppm (CH_3), 23.10–34.85 ppm (CH_2), 110.89–162.87 ppm (Ar−C), 162.47 ppm (C=N), 172.08 (C=O of ester).

Synthesis of o-n-hydroxy-p-n-hexadecanoyloxy-benzylidene-p-bromoaniline, 12

Yield 78%. Elemental analysis found: C, 65.45; H, 7.56; N, 2.60. Calculated (for $C_{29}H_{40}BrNO_3$): C, 65.65; H, 7.60; N, 2.64. IR (KBr), 3433 cm^{-1} (OH), 2952, 2917, 2847 cm^{-1} (C−H aliphatic), 1750 cm^{-1} (C=O of ester), 1615 cm^{-1} (CH=N), 1586 cm^{-1} (C=C aromatic). ^{1}H NMR ($CDCl_3$), 0.90–0.93 ppm (CH_3), 1.27–2.59 ppm (CH_2), 6.72–7.58 ppm (Ar−H), 8.56 ppm (CH=N), 13.14 ppm (OH). ^{13}C NMR ($CDCl_3$), 14.28 ppm (CH_3), 22.95–34.84 ppm (CH_2), 110.84–162.97 ppm (Ar−C), 162.47 ppm (C=N), 171.69 (C=O of ester).

Synthesis of o-n-hydroxy-p-n-hexadecanoyloxy-benzylidene-p-methoxyaniline, 13

Yield 74%. Elemental analysis found: C, 74.90; H, 9.12; N, 2.90. Calculated (for $C_{30}H_{43}NO_4$): C, 74.81; H, 9.00; N, 2.91. IR (KBr), 3444 cm^{-1} (OH), 2953, 2916, 2848 cm^{-1} (C−H aliphatic), 1758 cm^{-1} (C=O of ester), 1634 cm^{-1} (CH=N), 1605 cm^{-1} (C=C aromatic). ^{1}H NMR ($CDCl_3$), 0.91–0.95 ppm (CH_3), 1.32–2.59 ppm (CH_2), 3.85 ppm (OCH_3), 6.70–7.36 ppm (Ar−H), 8.58 ppm (CH=N), 13.59 ppm (OH). ^{13}C NMR ($CDCl_3$), 14.28 ppm (CH_3), 22.96–34.84 ppm (CH_2), 55.89 ppm (OCH_3), 110.69–162.87 ppm (Ar−C), 159.96 ppm (C=N), 171.78 (C=O of ester).

Synthesis of o-n-hydroxy-p-n-hexadecanoyloxy-benzylidene-p-methylaniline, 14

Yield 76%. Elemental analysis found: C, 77.46; H, 9.45; N, 2.99. Calculated (for $C_{30}H_{43}NO_3$): C, 77.38; H, 9.31; N, 3.01. IR (KBr), 3435 cm^{-1} (OH), 2952, 2917, 2848 cm^{-1} (C−H aliphatic), 1757 cm^{-1} (C=O of ester),

1627 cm^{-1} (CH=N), 1606 cm^{-1} (C=C aromatic). ^{1}H NMR ($CDCl_3$), 0.90–0.93 ppm (CH_3 of ester chain), 1.27–2.61 ppm (CH_2), 2.41 ppm (CH_3 of aniline fragment), 6.70–7.40 ppm (Ar−H), 8.62 ppm (CH=N), 13.74 ppm (OH). ^{13}C NMR ($CDCl_3$), 14.29 ppm (CH_3 of ester chain), 22.93–34.85 ppm (CH_2), 110.74–163.03 ppm (Ar−C), 161.14 ppm (C=N), 172.17 (C=O of ester).

Synthesis of o-n-hydroxy-p-n-hexadecanoyloxy-benzylidene-p-ethylaniline, 15

Yield 76%. Elemental analysis found: C, 77.65; H, 9.76; N, 2.91. Calculated (for $C_{31}H_{45}NO_3$): C, 77.62; H, 9.46; N, 2.92. IR (KBr), 3439 cm^{-1} (OH), 2953, 2916, 2847 cm^{-1} (C−H aliphatic), 1756 cm^{-1} (C=O of ester), 1628 cm^{-1} (CH=N), 1606 cm^{-1} (C=C aromatic). ^{1}H NMR ($CDCl_3$), 0.91–0.95 ppm (CH_3 of ester chain), 1.27–1.29 (CH_3 of aniline fragment), 1.32–2.61 ppm (CH_2 of ester chain), 2.68–2.74 ppm (CH_2 of aniline fragment) 6.70–7.39 ppm (Ar−H), 8.62 ppm (CH=N), 13.76 ppm (OH). ^{13}C NMR ($CDCl_3$), 14.56 ppm (CH_3 of ester chain), 16.02 ppm (CH_3 of aniline fragment), 23.14–34.86 ppm (CH_2 of ester chain), 28.89 ppm (CH_2 of aniline fragment), 110.80–162.98 ppm (Ar−C), 161.22 ppm (C=N), 172.10 (C=O of ester).

RESULTS AND DISCUSSION

Phase Transition Behavior and Liquid Crystallinity of Compounds 9–15

The phase transition temperatures and their associated enthalpy obtained from DSC analysis over heating and cooling cycles are tabulated in Table I. From Table I, it is clearly shown that upon heating all compounds except compounds **10**, **14**, and **15** exhibit endotherms characteristic of the crystal–mesophase and mesophase–isotropic transitions at temperatures greater than melting temperature (T_m). It is very clear that an endotherm that appeared over heating cycle for compound **14** suggests a direct melting from crystal-to-isotropic phase. However, the thermograms of compounds **10** and **15** have each shown an endotherm before the isotropization at 75 and 61°C, respectively. The texture observed under the polarizing microscope is indicative of the presence of subphases within the crystal phase (Cr_1-Cr_2) as those phenomena observed for isoflavone derivatives [19]. While the clearing points for compounds **9** and **12** represent the transition temperature of SmA-I, the clearing temperatures observed for compounds **10** and **15** at respective temperatures of 95°C and 86°C are merely for the crystal-isotropic phase transition. These

TABLE I Phase Transitions and Transition Enthalpy Changes For Compounds **9–15** upon Heating and Cooling

Compound	Phase transitions/°C (corresponding enthalpy change/Jg^{-1})	Heating/ cooling
9	Cr 68 (123) SmA 86 (15) I	
	I 64 (99) Cr	
10	Cr_1 75 (50) Cr_2 95 (100) I	
	I 88 (11) SmA 72 (133) Cr	
11	Cr_1 85 (75) Cr_2 110 (93) SmA 124 (16) I	
	I 124 (16) SmA 97 (92) Cr_2 77 (13) Cr_1	
12	Cr_1 70 (7) Cr_2 117 (76) SmA 128 (14) I	
	I 138 (15) SmA 110 (77) Cr_2 67 (6) Cr_1	
13	Cr 98 (109) SmA 111 (5) I	
	I 111 (5) SmA 78 (107) Cr	
14	Cr 93 (178) I	
	I 88 (5) SmC 83 (151) Cr	
15	Cr_1 61 (45) Cr_2 86 (101) I	
	I 82 (4) SmC 79 (92) Cr	

Cr_1 and Cr_2, crystal; SmA, smectic A; SmC, smectic C; I, isotropic.

phenomena could be ascribed to the increase of the melting point, which lies above the mesophase–isotropic liquid transition temperatures [20].

The data in Table I has also shown that upon cooling all compounds except compound **9** exhibit smectic phase. The cooling scan upon compound **11** shows the presence of mesophase (Figure 1(a)) with fan-shaped texture. This feature is characteristic of the SmA phase owing to the formation of batonnets that coalesce to form the fan-shaped texture [21]. The appearance of SmA phase is found to conform with analogue *p*-n-octadecanoyloxybenzylidene-*p*-chloroanilines (**18B-Cl**) as reported earlier [16]. One of the remarkable features is that the clearing temperature of compound **11** (124°C) is very much greater than compound **18B-Cl** (106°C) during heating cycle. This information indicates that the introduction of hydroxyl group at *ortho* position in the aldehyde fragment increases the degree of anisotropy of the molecular polarizability of compound **11** and hence increases the degree of molecular order causing the smectic phase to have increased stability [22]. A representative DSC thermogram of compound **11** during both heating and cooling scan is shown in Figure 2.

For compound **12**, the SmA with ellipses texture (Figure 1(b)) and SmA with fan-shaped texture (Figure 1(c)) were observed during heating and cooling, respectively. The smectic character of compound **12** is found to be similar to that reported in the literature [21].

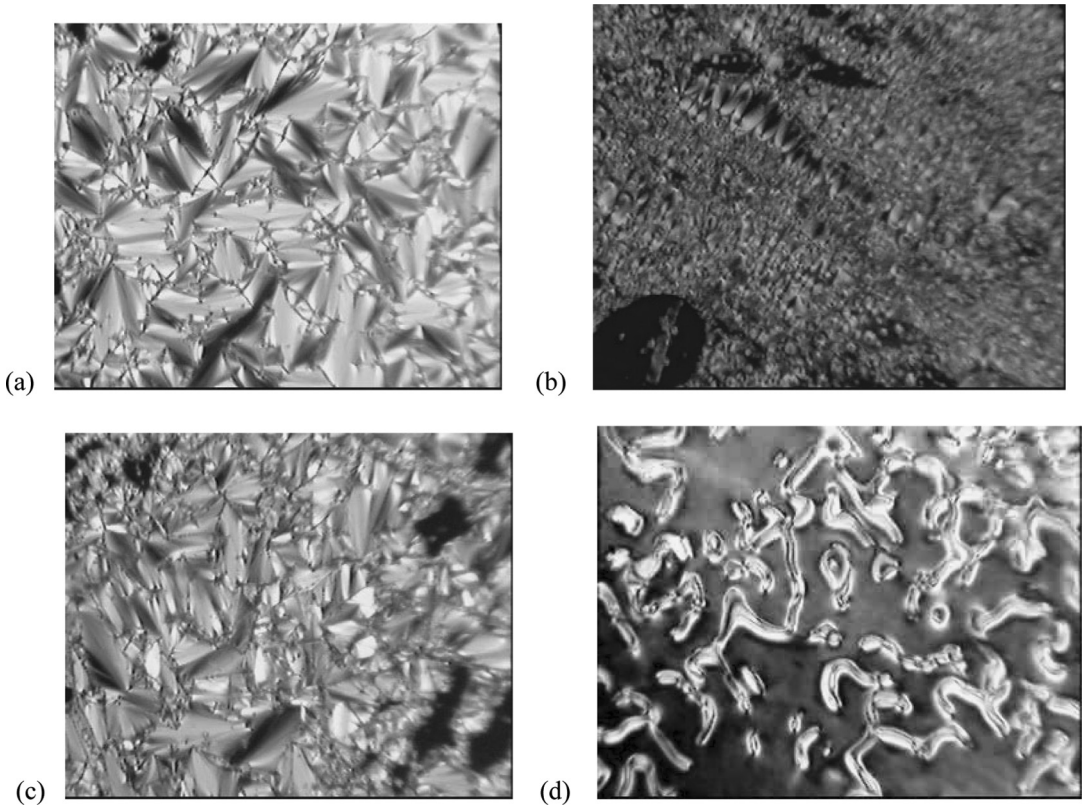

FIGURE 1 (a) Optical photomicrograph of compound **11** exhibiting smectic A with fan-shaped texture. (b) Optical photomicrograph of compound **12** exhibiting smectic A texture with ellipses. (c) Optical photomicrograph of compound **12** exhibiting smectic A with fan-shaped texture. (d) Optical photomicrograph of compound **14** exhibiting smectic C with *schlieren* texture. (See COLOR PLATE II).

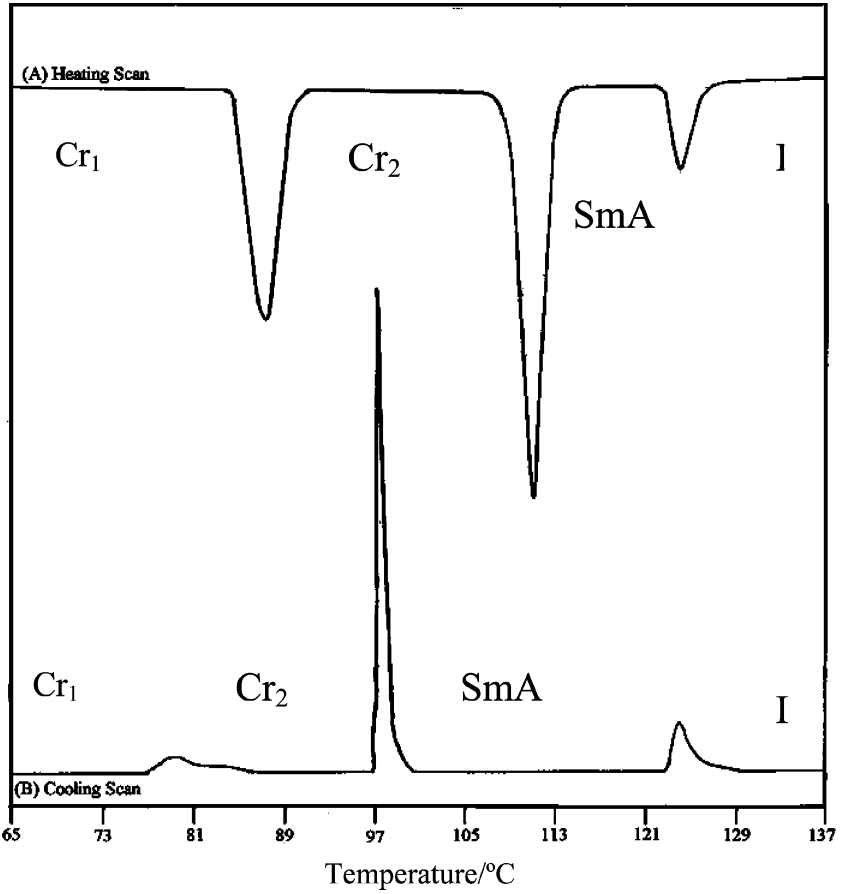

FIGURE 2 DSC thermograms of compound **11**.

The observation on compound **10** confirms the monotropic feature wherein the SmA phase appeared with fan-shaped texture during cooling cycle. Compounds **14** and **15**, which possess methyl and ethyl group in the respective aniline fragment, also exhibit monotropic properties. Both of these compounds upon cooling exhibit SmC phase at 88°C and 82°C, respectively. Figure 1(d) shows the optical photomicrograph of compound **14** exhibiting SmC with *schlieren* texture during cooling. One remarkable feature is that compound **14** possesses a higher clearing temperature in comparison with compound **15**. This phenomenon is similar with that reported by Artigas and coworkers [23], wherein the introduction of the hydroxyl group in the *ortho* position causes the mesophase stability to

TABLE II Polarizability (calculated value) for Compounds **9–15**

Compound	Polarizability (α, $\pm 0.5 \times 10^{-24}$)
9	54.33
10	54.28
11	56.16
12	57.33
13	56.64
14	56.09
15	57.09

favor for terminal chains of shorter length. As such, the compound with short terminal length is expected to possess a higher degree of molecular order, which is favored by the increase in the polarizabilty. This has been evident from the calculated polarizability values in which the polarizability of compound **14** is higher than compound **15** (Table II).

The influence of terminal group on mesophase stability can also be considered as one of the factors contributing towards the difference of temperature for transition from mesophase to isotropic phase. Among compounds **10–12**, wherein each compound possesses the halogen in the aniline fragment, the clearing temperature for compound **10** is very much lower in comparison with **12** and **13**. This comparison suggests that the fluorine (F) atom, which is the most electronegative, reduces the degree of molecular order despite the presence of hydroxyl group at *ortho* position. This thermal data also indicates that the influence of steric hindrance casued by the asymmetry of the central core of compound **10** is the least in comparison with compounds **12** and **13**, which possess higher clearing temperatures. This has also been confirmed by the polarizability values wherein the calculated polarizability (Table II) increases from compound **10** [$(54.28 \pm 0.5) \times 10^{-24}\,\mathrm{cm}^{-3}$] to compound **11** [[$(56.16 \pm 0.5) \times 10^{-24}\,\mathrm{cm}^{-3}$] and compound **12** [$(57.33 \pm 0.5) \times 10^{-24}\,\mathrm{cm}^{-3}$].

It needs to be pointed out that while the fluorine atom shows very low polarizability because the valence electrons residing at this atom are tightly held to the nucleus, bromine atom is considered larger than fluorine and hence is more easily polarized because electrons on this atom are far from the nucleus [24].

Influence of Lateral Polar Hydroxy Group on Mesomorphic Properties

This investigation has also revealed a correlation between the influence of lateral polar hydroxyl group on compounds **9–15** whereby a comparison

was made between the data of compounds **9**–**15** (Table I) and their analogues *p*-n-octadecanoyloxybenzylideneaniline (**18B-H**), -*p*-chloroaniline (**18B-Cl**), -*p*-methoxyaniline (**18B-OCH$_3$**), and -*p*-methylaniline (**18B-CH$_3$**) [16]. The clearing temperature of compounds **9** (86°C), **11** (124°C), **13** (111°C), and **14** (93°C) are found to be higher than those for compounds **18B-H** (78°C), **18B-Cl** (106°C), **18B-OCH$_3$** (104°C), and **18B-CH$_3$** (90°C), respectively.

It can therefore be assumed that the presence of an OH group in an *ortho* position in compounds **9–15** confers a higher degree of stability on the mesophase resulting from the increase in van der Waals forces, which in turn is caused by the increased anisotropy of the molecular polarizability.

Physical Characterization

The spectroscopic methods (FTIR, ^{1}H NMR, and ^{13}C NMR) have been employed to elucidate the target compounds (**9–15**). FTIR data show that the diagnostic bands assignable to the stretching of aliphatic C−H and carbonyl (C=O of ester) of compounds **9–15** were observed at the respective frequency ranges of 2847–2953 cm^{-1} and 1750–1759 cm^{-1}. The absorption bands appeared at higher frequency 3433–3444 cm^{-1} can be attributed to the stretching of O−H for compounds **9–15**. The absorption bands assignable to the stretching of C=N bond for compounds **9–15** were observed at frequency range of 1615–1634 cm^{-1}, and these values conform with those reported in the IR spectra for various substituted aromatic Schiff bases that possesses the formulation $HOC_6H_5CH{=}NC_6H_5$ [16].

^{1}H NMR data of compounds **9**–**15** show the presence of a singlet peak aasigned to the azomethine proton (CH=N) at the chemical shift $\delta = 8.56$–8.62 ppm. Compound **9** shows a triplet assignable to the methyl group of ester linkage at $\delta = 0.91$–0.94 ppm, and a multiplet that occurred at $\delta = 1.25$–1.27 ppm can be ascribed to methylene (CH_2) proton. The ^{1}H NMR spectrum of compound **9** also shows the presence of aromatic protons within the range of $\delta = 6.71$–7.46 ppm. Another singlet appeared at $\delta = 13.64$ ppm can be attributed to the hydroxyl (O−H) proton. The peaks with similar characteristics were also observed for compounds **10–15**. An additional peak occurring at $\delta = 3.85$ ppm can be attributed to the presence of methoxy (OCH_3) group in compound **13**. The structural information of compounds **9–15** can also be inferred from the ^{13}C NMR data, wherein a peak owing to the presence of ester carbonyl (−COO−) was observed within the range of $\delta = 171.69$–172.17 ppm, which is in agreement with those analogues earlier reported [16]. The appearance of a peak within the range of $\delta = 160.0$–162.5 ppm is due to the presence of the carbon in the imine (C=N) group in compounds **9–15**. An additional peak that appears at $\delta = 55.9$ ppm suggested the presence of the methoxy (OCH_3)

group. The results as inferred from the IR and NMR spectra suggest that the molecular structures for compounds **9–15** consist of two aromatic rings bridged by an imine group, which in turn forms an intramolecular hydrogen bonding (Scheme 1).

The formulations and molecular structures of compounds **9–15** are also supported by the microanalytical data wherein the percentages of C, H, and N thus found are in good agreement with the theoretical values, and the deviation of each result, in general, is not more than 0.3%. As such, the purity of each compound is considerably high, which entailed the subsequent thermal analysis and texture observation as we described in the earlier sections.

REFERENCES

[1] Sambanthamurthi, R., Sundram, K., & Tan, Y. I. (2000). *Prog. Lipid Res.*, *39*, 507–558.
[2] Ng, W. K., Tee, M. C., & Boey, P. L. (2000). *Aquacult. Res.*, *31*, 337–347.
[3] Ng, W. K., Lim, P. K., & Boey, P. L. (2003). *Aquaculture*, *215*, 229–243.
[4] Kuksis, A. & Beveridge, J. M. R. (1960). *J. Org. Chem.*, *25*, 1209–1219.
[5] Vogel, M. J., Barrall II, E. M., & Mignosa, P. (1970). *Liquid Crystals and Ordered Fluids*, Johnson, J. F. & Porter, R. S., (Eds.), Plenum Press: New York, p. 333–349.
[6] Gibson, H. W. & Pochan J. M. (1973). *J. Phys. Chem.*, *77*(6), 837–845.
[7] Craven, B. M. & Detitta, G. T. (1976). *J. C. S. Perkin II*, 814–822.
[8] Sawzik, P. & Craven, B. M. (1979). *Acta. Cryst.*, *B35*, 895–901.
[9] Puchkovskaya, G. A. & Yakubov, A. A. (1990). *J. Mol. Struct.*, *218*, 141–146.
[10] Yakubov, A. A. & Puchkovskaya, G. A. (1995). *J. Mol. Struct.*, *348*, 81–84.
[11] Rodriguez, C., Naito, N., & Kunieda, H. (2001). *Colloids Surf.*, *181*, 237–246.
[12] Filip, D., Simionescu, C. I., & Macocinschi, D. (2001). *Mater. Res. Bul.*, *36*, 1455–1461.
[13] Marcelis, A. T. M., Koudijs, A., Karczmarzyk, Z., & Sudhotler, E. J. R. (2003). *Liq. Cryst.*, *30*, 1357–1364.
[14] Hu, J. S., Zhang, B. Y., Sun, K., & Li, Q. Y. (2003). *Liq. Cryst.*, *30*, 1267–1275.
[15] Yeap, G. Y., Ha, S. T., Ito, M. M., Boey, P. L., & Mahmood, W. A. K. (2004). *J. Mol. Struct.*, *687*, 57–64.
[16] Yeap, G. Y., Ooi, W. S., Nakamura, Y., & Cheng, Z. (2002). *Mol. Cryst. Liq. Cryst.*, *381*, 169–178.
[17] Ooi, W. S. (2003). M. Sc. Thesis, Universiti Sains Malaysia, Malaysia.
[18] Sudhakar, S., Narasimhaswamy, T., & Srinivasan, K. S. V. (2000). *Liq. Cryst.*, *27*, 1525–1532.
[19] Belmar, J., Parra, M., Zuniga, C., Perez, C., Munoz, C., Omenat, A., & Serrano, J. L. (1999). *Liq. Cryst.*, *26*, 75–81.
[20] Gray, G. W. (1962). *Molecular Structure and the Properties of Liquid Crystals*, Academic Press: New York, p. 162.
[21] Demus, D. & Richter, L. (1978). *Textures of Liquid Crystals*, Verlag Chemie: New York.
[22] Collings, P. J. & Hird, M. (1998). *Introduction to Liquid Crystals*, Taylor & Francis Ltd.: London, UK.
[23] Artigas, M., Marcos, M., Melendez, E., & Serrano, J. L. (1985). *Mol. Cryst. Liq. Cryst.*, *130*, 337–347.
[24] Solomons, T. W. G. (1994). *Fundamentals of Organic Chemistry*, John Wiley & Sons, Inc: New York.